Journal of Alzheimer's Disease xx (20xx) x–xx
DOI 10.3233/JAD-150340
IOS Press

Looking for Neuroimaging Markers in Frontotemporal Lobar Degeneration Clinical Trials: A Multi-Voxel Pattern Analysis Study in *Granulin* Disease

Enrico Premi[a,e], Franco Cauda[b,c], Tommaso Costa[b,c], Matteo Diano[b,c], Stefano Gazzina[a], Vera Gualeni[a], Antonella Alberici[a], Silvana Archetti[d], Mauro Magoni[e], Roberto Gasparotti[f], Alessandro Padovani[a] and Barbara Borroni[a,*]

[a]*Centre for Ageing Brain and Neurodegenerative Disorders, Neurology Unit, Department of Clinical and Experimental Sciences, University of Brescia, Brescia, Italy*
[b]*GCS fMRI Koelliker Hospital, Turin, Italy*
[c]*Department of Psychology, University of Turin, Turin, Italy*
[d]*III Laboratory of Analyses, Azienda Ospedaliera "Spedali Civili", "Spedali Civili" Hospital, Brescia, Italy*
[e]*Stroke Unit, Azienda Ospedaliera "Spedali Civili", "Spedali Civili" Hospital, Brescia, Italy*
[f]*Neuroradiology Unit, Department of Surgery, Radiology and Public Health, University of Brescia, Brescia, Italy*

Accepted 1 December 2015

Abstract. In light of future pharmacological interventions, neuroimaging markers able to assess the response to treatment would be crucial. In *Granulin* (*GRN*) disease, preclinical data will prompt pharmacological trials in the future. Two main points need to be assessed: 1) to identify target regions in different disease stages and 2) to determine the most accurate functional and structural neuroimaging index to be used. To this aim, we have taken advantage of the multivariate approach of multi-voxel pattern analysis (MVPA) to explore the information of brain activity patterns in a cohort of *GRN* Thr272fs carriers at different disease stages (14 frontotemporal dementia (FTD) patients and 17 asymptomatic carriers) and a group of 33 healthy controls. We studied structural changes by voxel-based morphometry (VBM), functional connectivity by assessing salience, default mode, fronto-parietal, dorsal attentional, executive networks, and local connectivity by regional homogeneity, amplitude of low frequency fluctuations (ALFF), fractional ALFF (fALFF), degree centrality, and voxel-mirrored homotopic connectivity. In FTD patients with *GRN* mutation, the most predictive measure was VBM structural analysis, while in asymptomatic carriers the best predictor marker was the local connectivity measure (fALFF). Altogether, all indexes demonstrated fronto-temporo-parietal damage in *GRN* pathology, with widespread structural damage of fronto-parietal and temporal regions when disease is overt. MVPA could be of aid in identifying the most accurate neuroimaging marker for clinical trials. This approach was able to identify both the target region and the best neuroimaging approach, which would be specific in the different disease stages. Further studies are needed to simultaneously integrate multimodal indexes in a classifier able to trace the disease progression moving from preclinical to clinical stage of the disease.

Keywords: Degree centrality, fractional amplitude of low frequency fluctuation, frontotemporal dementia, *granulin*, multi-voxel pattern analysis, regional homogeneity, resting state fMRI, support vector machine learning, voxel-mirrored homotopic connectivity

*Correspondence to: Barbara Borroni, MD, Neurology Unit, University of Brescia, Piazza Spedali Civili 1, Brescia 25125, Italy. E-mail: bborroni@inwind.it.

INTRODUCTION

Frontotemporal lobar degeneration (FTLD) is an heterogeneous group of diseases characterized by prominent frontal and behavioral features [1, 2]. Different clinical phenotypes have been described, i.e., the behavioral variant frontotemporal dementia (bvFTD), the agrammatic variant of primary progressive aphasia (avPPA), and the semantic variant of PPA (svPPA) [1, 2]. For each clinical phenotype, specific neuroimaging patterns have been identified [3, 4]. Neuropathologically, in most of cases, frontotemporal dementia (FTD) is characterized by either Tau (FTLD-Tau) or TAR-DNA-binding protein-43 (TDP-43) (FTLD-TDP) inclusions [5]. In the last two decades, a number of autosomal dominant causative mutations, such as mutations within *Microtuble Associated Protein Tau* (*MAPT*) and *Granulin* (*GRN*) along with repeat expansion of *C9orf72* gene [6, 7] have been described.

In particular, in *GRN* mutation cases, clinical presentation can be heterogeneous, ranging from typical bvFTD to avPPA, but also with some cases resampling corticobasal syndrome [8]. From this point of view, if the asymmetric fronto-temporo-parietal atrophy and functional impairment within salience network and fronto-parietal network have been defined [8, 9], neuroimaging pattern of alteration can be quite different considering the different clinical phenotypes of *GRN* mutations [10]. Multivariate statistical approach (like multi-voxel pattern analysis, MVPA) to neuroimaging data has received increasing attention, allowing the possibility to explore correlation/covariance pattern of activation between brain regions with greater statistical power, overcoming the classical univariate statistical inference of voxel-by-voxel analysis, by stringent correction for voxelwise multiple comparisons [11]. MVPA [12, 13] represents a promising approach to study the information that is represented in different patterns of neural activity, through the application of an automated classifier (i.e., support vector machine, SVM) [14] to capture the complex relationships among spatial pattern of brain activity in the studied populations [15]. From this perspective, monogenic FTD represents a privileged point of view to test the potential role of disease-modifying therapies, as cases with known neuropathology and following the continuum from presymptomatic to symtomatic stages [16, 17]. As recently demonstrated by GENFI initiative [17], *GRN* carriers are characterized by insular and parietal structural alteration up to 15 years before the clinical onset, supporting the pivotal role of specific preclinical biomarker to trace neurodegenerative diseases like FTD and AD [18]. In light of future disease modifying therapies, neuroimaging markers able to assess the response would be key [17], with the ideal marker should respond not only to the region that needs to be investigated, but also in which way. In the present work, we applied the multivariate approach of MVPA to different magnetic resonance imaging (MRI) metrics to study *GRN*-related disease (asymptomatic subjects carrying *GRN* Thr272fs mutation and FTD patients bearing the same mutation): voxel-based morphometry (VBM, for structural grey and white matter alterations) [19] and a series of functional network connectivity measures. First of all, we explored different brain functional networks by independent component analysis (ICA), considering the involvement of specific networks in FTD related to *GRN* [20]. More recently, a number of functional parameters has been used to study local properties of brain activity at rest, also in FTD related to *GRN*, like regional homogeneity (ReHo), to look at the coherence of focal resting state fluctuations [21], the fractional amplitude of low frequency fluctuation (fALFF, that describes the power of the signal in the low frequency range) [22], degree centrality (DC, that allows the study of the nodes that form the whole-brain network [23], and the voxel homotopic connectivity (VMHC, as index of functional symmetry in resting-state brain activity) [24]. In the present work we have taken advantage of the multivariate approach as machine-learning classifier of MVPA: 1) to identify the most accurate functional and/or structural neuroimaging index to be used, and 2) to define the most accurate neuroimaging pattern to classify the different stages of the *GRN* disease.

METHODS

Subjects

Subjects were recruited at the Centre for Ageing Brain and Neurodegenerative Disorders, University of Brescia (Brescia, Italy). The studied sample included 64 subjects. 14 were patients with FTD carrying *GRN* Thr272fs mutation (FTD-*GRN*+), and 16 of them were age and gender-matched healthy subjects (old healthy controls, oHC). Furthermore, 17 asymptomatic carriers carrying *GRN* Thr272fs mutation (a*GRN*+) and 17 non-carriers belonging to the same families (young healthy controls, yHC) were recruited (see Supplementary Figure 1).

FTD patients met current clinical diagnostic criteria either for bvFTD (7 cases) or avPPA (7 cases)

[1, 2]. An extensive neuropsychological assessment in both patients and asymptomatic siblings, including the FTD-modified Clinical Dementia Rating scale (FTD-modified CDR) was administered, as previously described [25].

Written informed consent from the subject or from the responsible guardian if the subject was incapable, was obtained, for each procedure, before study initiation, as well as for blood collection by venous puncture, genetic analysis, and MRI scanning. The research protocol was approved by the ethics committee of the Brescia Hospital. The work conformed to the Helsinki Declaration.

Granulin sequencing

Genomic DNA was extracted from peripheral blood using a standard procedure. All the 12 exons plus exon 0 of *GRN*, and at least 30 base pairs (bp) of their flanking introns were evaluated by polymerase chain reaction (PCR) and subsequent sequencing. *GRN* Thr272fs (g.1977_1980 delCACT) was tested as described elsewhere [26].

MRI acquisition

All imaging was obtained using a 1.5T Siemens Symphony magnetic resonance scanner (Siemens, Erlangen, Germany), equipped with a circularly polarized transmit-receive coil. In a single session, the following scans were collected from each studied subject: 1) Dual-echo turbo spin echo (TSE) (repetition time [TR] = 2500 ms, echo time [TE] = 50 ms), to exclude the presence of macroscopic brain abnormalities, according to exclusion criteria; 2) 3D magnetization-prepared rapid gradient echo (MPRAGE) T1-weighted scan (TR = 2010 ms, TE = 3.93 ms, matrix = $1 \times 1 \times 1$, in-plane field of view [FOV] = 250×250 mm^2, slice thickness = 1 mm, flip angle = 15°); and (3) T2*-weighted echo planar (EPI) sensitized to blood oxygen level dependent (BOLD) contrast (TR = 2500 ms, TE = 50 ms, 29 axial slices parallel to anterior commisure–posterior commissure line (AC-PC) line, matrix = 64×64, field of view = 224 mm, slice thickness = 3.5 mm) for resting state fMRI. Blood oxygen level dependent EPI images were collected during rest for an 8-min period, resulting in a total of 195 volumes. During this acquisition, subjects were instructed to keep their eyes closed, not to think of anything in particular, and not to fall asleep.

MRI preprocessing

As previously described [16, 20], all preprocessing steps were carried out using Advanced Data Processing Assistant for resting-state fMRI (DPARSFA) (http://rfmri.org/DPARSF) [27] which is based on Resting-State fMRI Data Analysis Toolkit (REST, http://www.restfmri.net) [28] and Statistical Parametric Mapping (SPM8) (http://www.fil.ion.ucl.ac.uk/spm). Grey matter (GM) and white matter (WM) probability maps using SPM5 Unified Segmentation were calculated, applying a spatial smoothing with an isotropic Gaussian kernel (full-width at half-maximum (FWHM), $10 \times 10 \times 10$ mm) to reduce spatial noise. For resting state fMRI analysis (ICA networks and local connectivity measures) all data were spatially normalized to the T1 unified segmentation template in Montreal Neurological Institute coordinates derived from SPM8 software and resampled to $3 \times 3 \times 3$ cubic voxels. For all considered measures, a spatial smoothing (FWHM = $8 \times 8 \times 8$ mm) was applied to reduce spatial noise. ICA functional brain networks, i.e., the salience (SN), the default mode (DMN), the fronto-parietal (FPN), the dorsal attentional (DAN), the executive (EN) networks were obtained. Moreover, local connectivity network measures, i.e., ReHo, ALFF, fALFF, DC, and VMHC, were computed. For each subject, all the derived voxelwise whole-brain maps (either structural (GM and WM) and functional (ICA networks, ReHo, ALFF, fALFF, DC, VMHC)) were considered for MVPA analysis.

Dimensionality reduction

Before MVPA analysis we need a dimensionality reduction of the data. The dimensionality problem, i.e., the number of voxels greater than the number of subjects, implies that the dataset is ill-conditioned, thus, not guaranteeing the existence of a unique solution. For this reason, we then reduced the computational complexity of the classification representing the data in a space of smaller dimensionality. First, we created a series of masks by performing t tests ($T < 0$, $p < 0.05$ FDR corrected) between all neuroimaging measures across participants within a classification comparison (FTD-*GRN*+ and oHC; *aGRN*+ and yHC). Then we used the singular value decomposition (SVD) to further reduce the dimensionality of all the data [29]. The SVD seek for an orthogonal basis that explained most of the variance of the data. By projecting the original data on the principal components, the set of correlated variables (voxels) were transformed into a set of

uncorrelated variables that were a linear combination of the original variables. Defining a N (subjects) × M (voxels) mean centered matrix, the SVD searched the eigenvalues and eigenvectors of the (M × M) covariance matrix. Because the number of voxels M exceeded the number of subjects N, there were only N–1 significant eigenvectors. The final results of the SVD is a matrix of dimension N × N.

Multivoxel pattern analysis (MVPA)

MVPA has gained increasing interest because it allows the detection of differences between conditions by focusing on the analysis and comparison of distributed spatial patterns of activity [30]. In order to inspect if the different types of maps (i.e., structural maps such as GM and WM probabilistic voxelwise maps) as well as functional maps (i.e., ICA-based network and local connectivity indexes) had statistically significant discrimination capacity, we employed a SVM approach [29]. This can be considered a supervised classification problem where a classifier attempts to capture the relationships between spatial patterns of fMRI activity and experimental conditions, assigning the fMRI activity of each subject to one of several predefined conditions (for example, FTD-*GRN*+ versus oHC) using a set of examples of the same fMRI activity. To make this decision we used the leave one out method with the experimental data.

Classifier

To verify the existence of multivariate differences in the studied comparisons (FTD-*GRN*+ versus oHC and *aGRN*+ versus yHC) we treated each map as a point in a multidimensional space (number of principal components), the result of the linear classification was equivalent to search the hyperplane that separated the two classes. This hyperplane was a linear function that was able to separate the data defined as:

$$w^T v + b = 0$$

where w is the weight vector, b was the intercept (offset) and v the volumes projected on the principal components. This hyperplane was learned during the training phase, and corresponds to a decision function that can be used to classify the examples used in the test phase. In our case, the algorithm used to find the hyperplane of separation between the two classes was the algorithm proposed by Boser et al. [31], also known as SVM [29, 32]. The weight vectors and the intercept determined the separation hyperplane. If the samples were in the voxels space, the weight vector w represented a volume with the most discriminant regions. This means that given two classes that represent the two experimental conditions, a positive voxel value indicates that the voxel has greater activity during condition 1 compared to condition 2 in most of training examples, and a negative voxel value indicates more reduced activity in condition 1 compared to condition 2. Since the classifier was multivariate in nature, the combination of all discriminant voxels, as a whole, was identified as a global activation pattern in which the brain states differ. The absolute value of each element of the map, obtained by discriminant classifier, determined its importance.

Furthermore, it was possible to obtain a probabilistic map of the most discriminative voxels. This was done using a statistical non-parametric methods. This step tested the hypothesis that there was no difference between the two brain states of the two classes using a permutation test of the label of the two classes and training the SVM with this permutation of labels. In this way, we estimated a probability distribution of each voxel under the assumption that there was no relationship between the label of the class. We achieved a voxel level p statistic (proportion of values in the distribution). For a given voxel, if p was significantly small, then the voxel discriminates between the two classes. In this sense, positive (increased, red to yellow) and negative (reduced, blue to green) areas should not be strictly considered as an absolute change of the studied parameter (for example GM density), but only as areas with significantly greater information to classify a subject as patients (i.e., FTD-*GRN*+) or healthy controls (i.e., oHC).

Classifier performance

To evaluate the performance of the classifier, we used a leave-one-subject-out cross validation test [33], considered a valid approach with scarce data [34]. In each learning phase, given the set of S subjects, one example was left out and the S-1 remaining examples were used as training set. After the learning phase, in the test phase, the excluded subject was used to assess the performance of the machine. This procedure was repeated S times, once for each excluded subject. The result was an average performance of the different trained machines. Furthermore, for each studied index (structural and functional) sensitivity and specificity were defined. Finally, for each studied subject,

misclassification (i.e. how many indexes correctly classified that specific subject) was considered.

All calculations were made using the LIBSVM library by Chang et al. [35] and in house developed Matlab scripts.

Statistical analysis

SPSS package (v. 21.0, Chicago, IL, USA) was employed to run statistics for group differences in demographic and clinical characteristics. Group comparisons were assessed by Mann-Whitney test or χ^2 test, setting the statistical threshold to p-values Bonferroni's corrected ≤ 0.05.

RESULTS

Demographic, clinical and neuropsychological characteristics of the studies subjects were reported in Table 1. See Supplementary Table 1 for the neuropsychological evaluation of FTD-*GRN*+ patients.

We inspected whether the different anatomical measures and the different patterns of functional connectivity were able to classify the two pathological categories compared to healthy controls groups (FTD-*GRN*+ versus oHC and *aGRN*+ versus yHC) correctly. For each group, we calculated a series of voxelwise anatomical (GM and WM) and functional measures related to local connectivity (DC, ALFF, fALFF, ReHo, VMHC) and to ICA networks (SN, DMN, EN, FPN, DAN). Figure 1A showed a graph depicting the classification performances and the related table with the accuracy for each studied measures; Fig. 1B reported, for each subject, the number of measures with a correct classification (true positive). Classification performance was significantly lower in FTD-*GRN*+ compared to oHC (8.9 ± 3.2 versus 11.4 ± 2.5, $p = 0.025$, Mann Whitney U test). Interestingly, the four patients with the smallest number of correct classifications (patient 1 = 6; patient 6 = 3; patient 11 = 6; patient 14 = 4) were all affected by agrammatic variant of PPA. In this sense, the inclusion of both clinical phenotypes of GRN disease partially reduced homogeneity and could explain the difference in classification performances. No significant differences between *aGRN*+ and yHC (6.8 ± 2.0 versus 6.8 ± 1.5, $p = 0.93$, Mann Whitney U test). Sensitivity and specificity for all the studied measures are reported in Table 2. As expected, the FTD-*GRN*+ versus oHC comparison showed better classification performances than *aGRN*+ versus yHC. GM atrophy (with left frontal, temporal, and parietal pattern) raised the greatest values, correctly classifying 96.5% of FTD-*GRN*+; even white matter bundle alterations were good predictors of FTD-*GRN*+ pathology, with the more discriminative tracts localized in fronto-temporal regions (uncinate fasciculus, anterior commissure and inferior longitudinal fasciculus). The high overlap between blue-green areas (classifying for FTD-*GRN*+ group) and known atrophic regions in FTD-*GRN*+ (in line with literature data) [4, 10], supported the concept that atrophic regions in FTD-*GRN*+ contained the highest information to correctly classify an FTD-*GRN*+ subject. On the other hand, red-yellow areas should not be considered as areas with "increased" GM density in FTD-*GRN*+, but only as areas with the highest predictive value for oHC in MVPA analysis.

In regard to functional measures, all local connectivity measures, such as DC, ALFF, fALFF, ReHo, and VMHC showed good discrimination power in identifying FTD-*GRN*+ (79.3–82.8%). Even with some slight differences among measures, the best discriminative pattern for local connectivity indexes was characterized by a reduced connectivity in the frontal, temporal, and parietal regions with a concomitant increased connectivity in the surrounding regions (Fig. 2). Considering ICA networks, ventral SN and left FPN showed the highest classification performances

Table 1
Clinical and demographic characteristics of included subjects

Variable	*FTD-GRN*+ ($n = 14$)	*oHC* ($n = 16$)	*aGRN*+ ($n = 17$)	*yHC* ($n = 17$)	*p*
Age at evaluation, y	60.4 ± 5.3	59.7 ± 8.7	41.6 ± 9.0	36.3 ± 7.4	n.s.*
Age at onset, y	58.8 ± 6.2	–	–	–	
Disease duration, y	1.93 ± 1.9	–	–	–	
Gender, female % (*n*)	64.3 (9)	75.0 (12)	47.1 (8)	64.7 (11)	n.s.^
Family history, positive % (*n*)	85.7 (12)	–	100 (17)	–	
Clinical phenotype, bvFTD % (*n*)	50.0 (7)	–	–	–	
Educational level, y	7.5 ± 2.6	9.1 ± 4.6	11.2 ± 3.8	11.6 ± 3.4	n.s.*

FTD, frontotemporal dementia; FTD-*GRN*+, FTD patients carrying *Granulin* Thr272fs mutation; oHC, old healthy controls; a*GRN*+, asymptomatic subjects carrying *Granulin* Thr272fs mutation; yHC, young healthy controls; FTD-CDR, frontotemporal dementia modified Clinical Dementia Rating scale. *Mann-Whitney U test (FTD-*GRN*+ versus oHC and *aGRN*+ versus yHC); χ^2 test (FTD-*GRN*+ versus oHC and *aGRN*+ versus yHC).

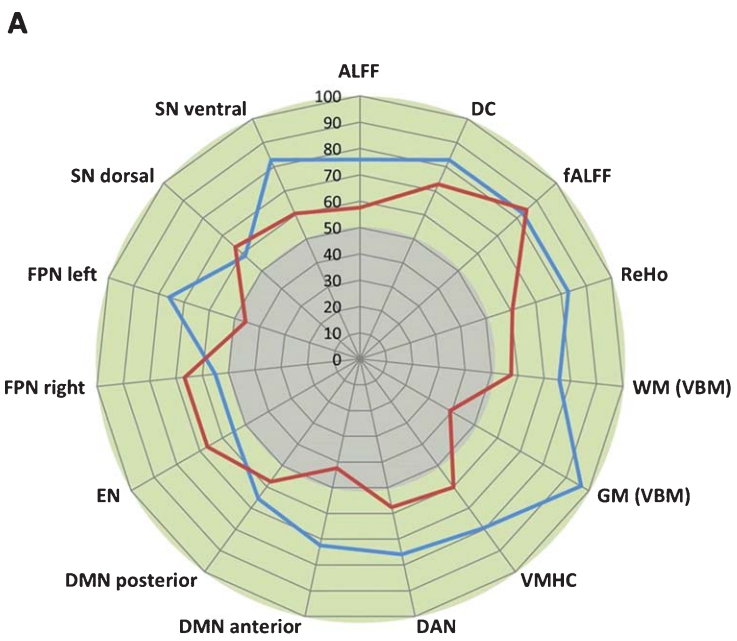

	FTD-*GRN*+ vs oHC	*aGRN*+ vs yHC
GM (VBM)	96,5	39,4
WM (VBM)	75,8	57,5
ALFF	75,9	57,6
fALFF	82,8	84,8
DC	82,8	72,7
ReHo	82,8	60,6
VMHC	79,3	60,1
DAN	75,8	57,5
DMN anterior	72,4	42,4
DMN posterior	65,5	57,6
EN	55,1	66,7
FPN right	55,1	66,7
FPN left	75,9	45,5
SN dorsal	58,6	63,6
SN ventral	82,8	60,6

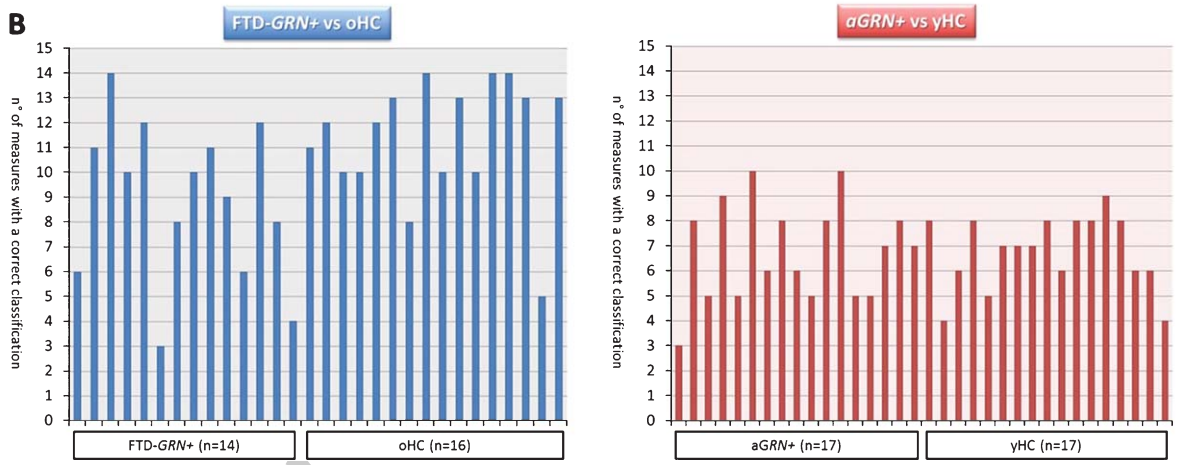

Fig. 1. A) Radar chart showing the classification results (discriminative power) of the different structural and functional measures. The green ring represents the significant (>55% of right classification) performance for each measure. Blue line is for FTD-*GRN*+ versus oHC and red line is for *aGRN*+ versus yHC. On the right, a table with the discriminative power (accuracy) of each studied measure is reported. B) Bar graphs with the number of measures with a correct classification (true positive) for each studied subject, considering FTD-*GRN*+ versus oHC (blue) and *aGRN*+ versus yHC (red); the overall number of measures was 15. FTD-*GRN*+, frontotemporal dementia carrying *Granulin* mutation; *aGRN*+, asymptomatic carriers of *Granulin* mutation; oHC, old healthy controls; yHC, young healthy controls; GM, grey matter; WM, white matter; VBM, voxel based morphometry; SN, salience network; DMN, default mode network; FPN, fronto-parietal network; DAN, dorsal attentional network; EN, executive network; ReHo, regional homogeneity; ALFF, amplitude of low frequency fluctuations; fALFF: fractional amplitude of low frequency fluctuations; DC, degree centrality; VMHC, voxel-mirrored homotopic connectivity.

between FTD-*GRN*+ versus oHC (82.8% and 75.9%), with a spatial pattern of frontal-temporal and parietal reduction, with areas of increased connectivity in left frontal cortex (left FPN).

In *aGRN*+, structural indexes (GM and WM density) were not able to classify *aGRN*+ subjects (GM: 39.4% and WM: 57.5%). Otherwise, the best classification performances were obtained by functional

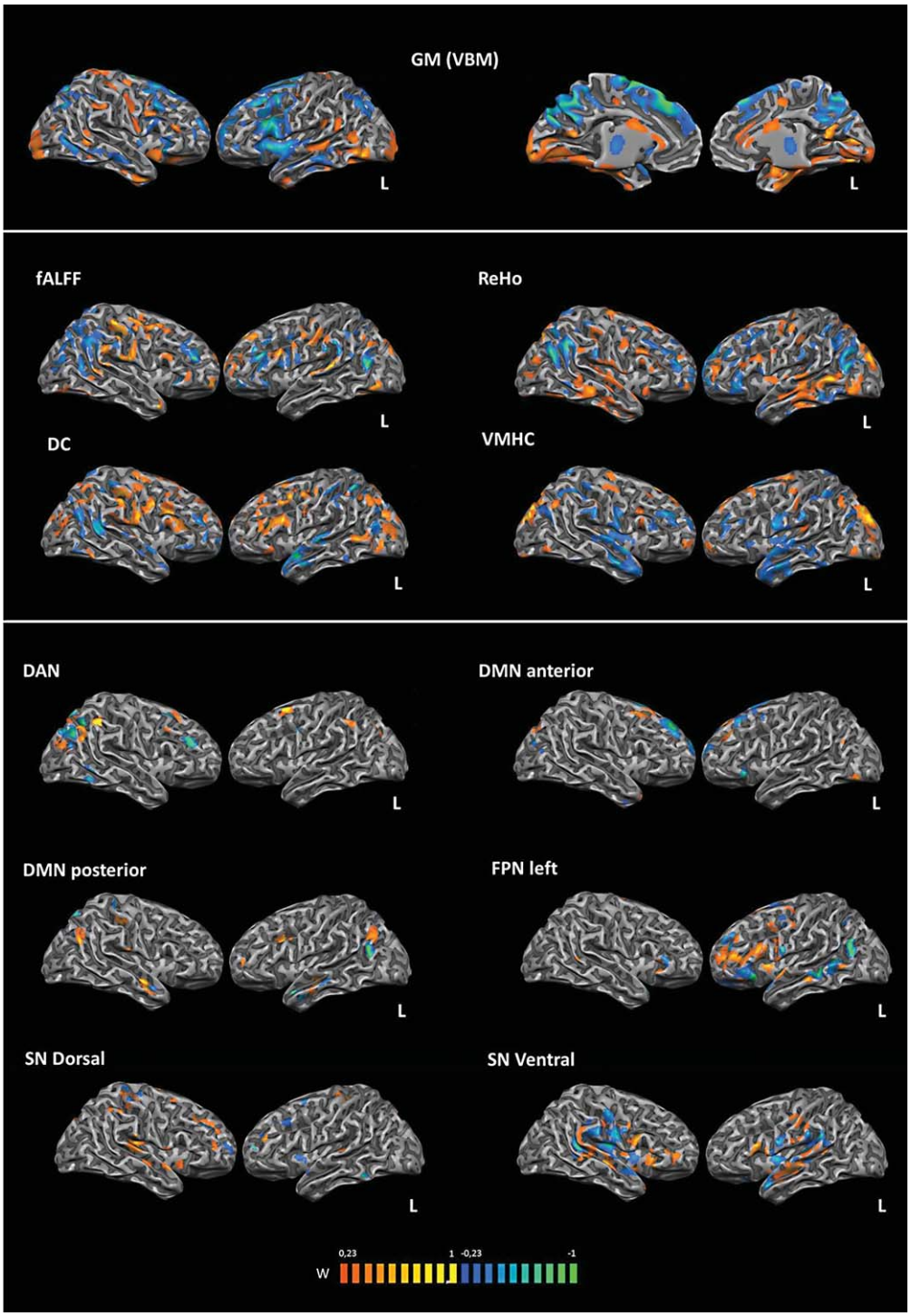

Fig. 2. Significant anatomical, voxelwise functional and network-related discriminative patterns for the FTD-*GRN*+ versus oHC. Blue to green are areas with "reduced" activity that predict for FTD-*GRN*+, red to yellow are areas with "increased" activity that predicts for FTD-*GRN*+. All significant results are superimposed on a 3D T1 MRI anatomical template. FTD-*GRN*+, frontotemporal dementia carrying *Granulin* mutation; *aGRN*+, asymptomatic carriers of *Granulin* mutation; oHC, old healthy controls; yHC, young healthy controls; GM, grey matter; WM, white matter; VBM, voxel based morphometry; SN, salience network; DMN, default mode network; FPN, fronto-parietal network; DAN, dorsal attentional network; EN, executive network; ReHo, regional homogeneity; ALFF, amplitude of low frequency fluctuations; fALFF: fractional amplitude of low frequency fluctuations; DC, degree centrality; VMHC, voxel-mirrored homotopic connectivity.

Table 2
Standard deviation, sensitivity and specificity of classifier performances across the leave-one-out validation in the studied groups and imaging modalities

	FTD-*GRN*+ versus oHC			*aGRN*+ versus yHC		
	SD	Sensitivity	Specificity	SD	Sensitivity	Specificity
GM (VBM)	4.9	0.86	0.99	6.1	0.23	0.41
WM (VBM)	6.3	0.78	0.87	9.9	0.52	0.52
ALFF	7.6	0.5	0.75	5.7	0.41	0.29
fALFF	4.7	0.71	0.75	8.6	0.76	0.52
DC	9.7	0.78	0.87	6.8	0.58	0.58
ReHo	3.6	0.71	0.93	6.3	0.41	0.47
VMHC	5.4	0.43	0.93	6.4	0.35	0.52
DAN	7.7	0.71	0.68	10.9	0.35	0.41
DMN anterior	7.2	0.71	0.68	4.9	0.35	0.29
DMN posterior	5.6	0.42	0.75	5.9	0.35	0.35
EN	5.2	0.28	0.5	10.4	0.47	0.47
FPN right	5	0.28	0.37	7.2	0.64	0.58
FPN left	7.3	0.64	0.68	5.3	0.29	0.35
SN dorsal	7.1	0.28	0.62	10.8	0.41	0.41
SN ventral	5.7	0.64	0.93	4.1	0.52	0.52

FTD-*GRN*+, frontotemporal dementia carrying *Granulin* mutation; *aGRN*+, asymptomatic carriers of *Granulin* mutation; oHC, old healthy controls; yHC, young healthy controls; SD, standard deviation; GM, grey matter; WM, white matter; VBM, voxel-based morphometry; ALFF, amplitude of low frequency fluctuations; fALFF, fractional amplitude of low frequency fluctuations; DC, degree centrality; ReHo, regional homogeneity; VMHC, voxel-mirrored homotopic connectivity; DAN, dorsal attentional network; DMN, default mode network; EN, executive network; FPN, fronto-parietal network; SN, salience network.

measures (fALFF: accuracy: 84.8%, sensitivity: 76%, specificity: 52%; and DC; accuracy: 72.7%, sensitivity: 58%, specificity: 58%). The best discriminative pattern for local connectivity indexes presented a reduced connectivity in posterior regions and increased connectivity in prefrontal regions (Fig. 3). ICA networks presented an overall low discrimination power, with the best performances for the right FPN, EN and ventral SN (66.7%, 66.7% and 63.6%) (Figs. 1 and 3). A high spatial concordance between ventral SN and right FPN was evident especially in the inferior frontal regions; otherwise, EN presented a pattern of increased connectivity in prefrontal regions, accordingly with local connectivity findings (Figs. 1 and 3).

As summarized in Fig. 4 (overlap of classification areas across all the measures here employed between FTD-*GRN*+ versus oHC (Fig. 4A) and *aGRN*+ versus yHC (Fig. 4B)), the best predictive measure to distinguish FTD-*GRN*+ from oHC was VBM GM density, with the more discriminative pattern involving frontal-temporal and parietal regions (and, in particular, left frontal and parietal among all, by areas). Conversely, *aGRN*+ group was better classified by local connectivity measures (especially fALFF) with a discrimination pattern characterized by a widespread connectivity decrease in parietal and posterior associative areas, with a well-structured increased connectivity in prefrontal regions. Especially for *aGRN*+ and in line with literature data [16, 20, 36], the concept that red-yellow areas could be considered as increased connectivity was more plausible. Finally, fALFF index was the only measure with high (>80%) discriminative power in both comparisons (FTD-*GRN*+ versus oHC and *aGRN*+ versus yHC).

DISCUSSION

In the last years, considerable steps forward in the knowledge of the pathogenesis of FTD have been made [7, 37], principally based on the identification of neuropathological inclusions and inherited determinants of the disease [38–40]. In this sense, the study of the monogenic forms of FTLD, such as *GRN*, *MAPT* or *C9orf72* [41, 42], represents the ideal experimental model to define markers related to a specific molecular pathway [6, 17, 43]. *GRN* mutations lead to a homogeneous FTD-TDP pathology and give the opportunity to unravel FTD from asymptomatic to symptomatic stages [17, 20, 44]. The definition of surrogate endpoints will be mandatory to test the efficacy of future pharmacological treatments [17].

MRI represents one of the most powerful tools to study *in vivo* neurodegenerative disorders, with a wide range of possible sequences, and to explore in depth brain functional and structural abnormalities [17, 45]. However, in FTD spectrum, and in *GRN* disease in particular, it is still unknown which target brain patterns might be the most sensitive to capture the ongoing neuropathological process in both pre-symptomatic and symptomatic disease phases, and which MRI technique

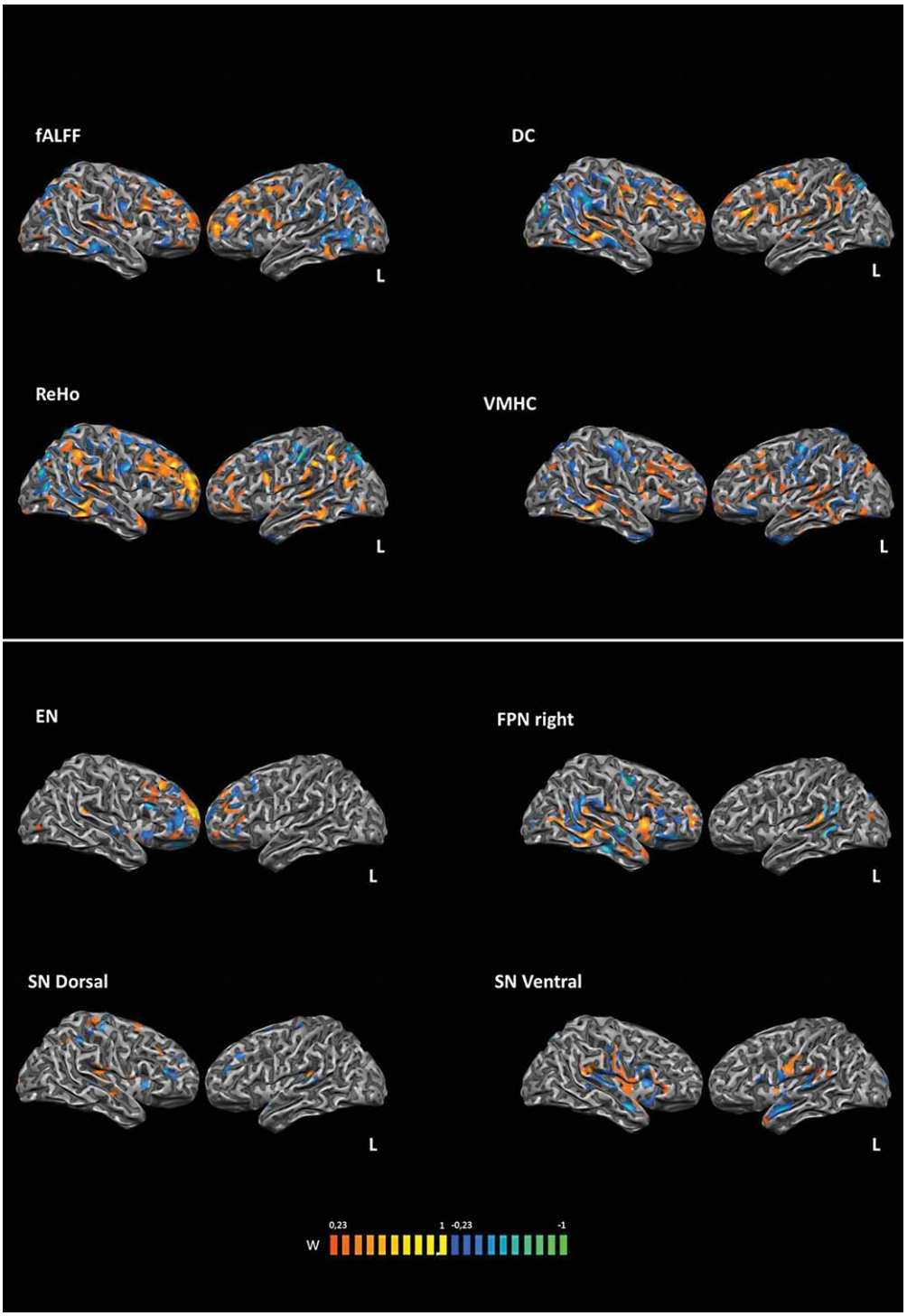

Fig. 3. Significant anatomical, voxelwise functional and network-related discriminative patterns for the a*GRN*+ group versus yHC. Blue to green are areas with "reduced" activity that predicts for a*GRN*+, red to yellow are areas with "increased" activity that predicts for a*GRN*+. All significant results are superimposed on a 3D T1 MRI anatomical template. *aGRN*+, asymptomatic carriers of *Granulin* mutation; oHC, old healthy controls; yHC, young healthy controls; SN, salience network; DMN, default mode network; FPN, fronto-parietal network; DAN, dorsal attentional network; EN, executive network; ReHo, regional homogeneity; ALFF, amplitude of low frequency fluctuations; fALFF: fractional amplitude of low frequency fluctuations; DC, degree centrality; VMHC, voxel-mirrored homotopic connectivity.

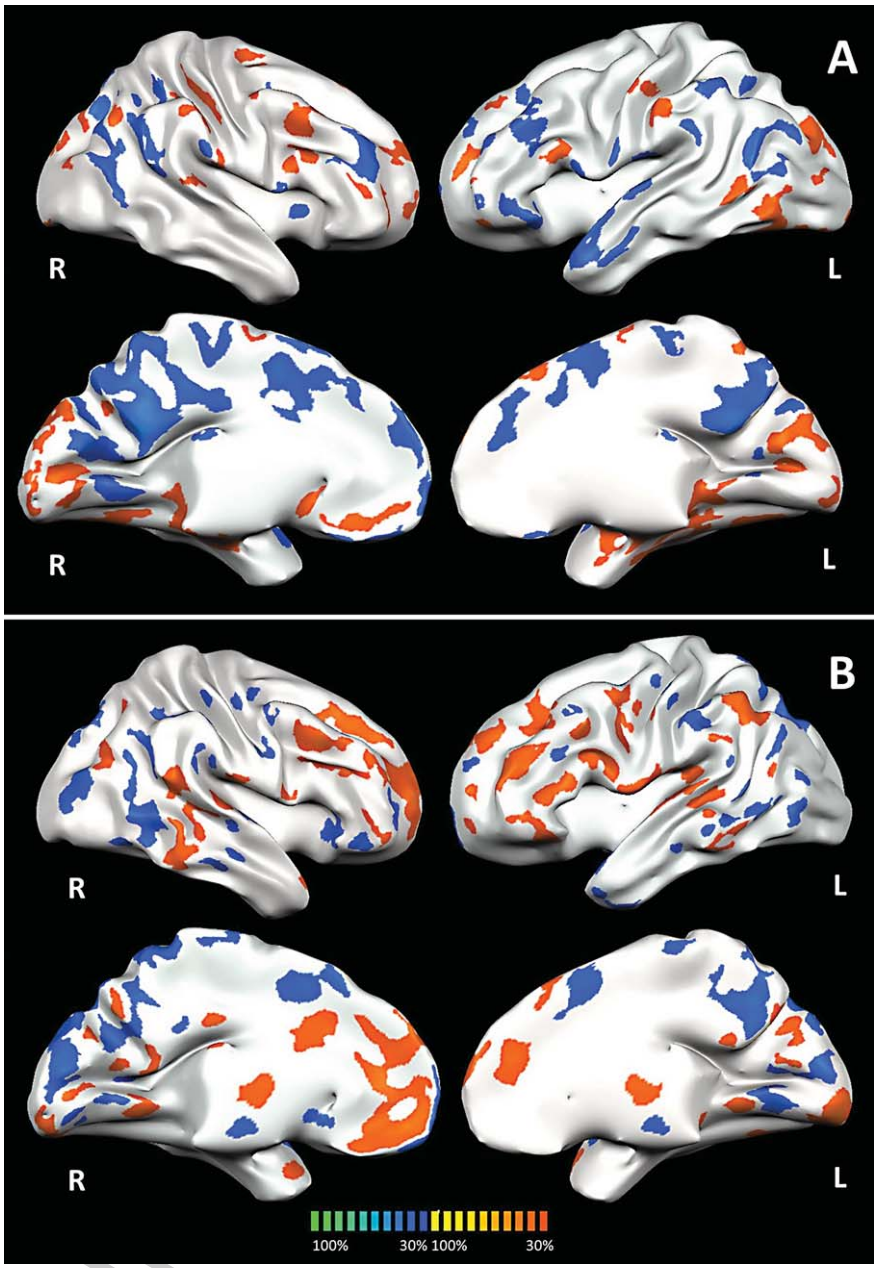

Fig. 4. Probabilistic maps with the areas with the highest cumulative predictive weights for all the measures. A) FTD-*GRN*+. B) *aGRN*+. Blue to green are areas with "reduced" activity that predict for the pathological sample, red to yellow are areas with "increased" activity that predict for the pathological sample. These images shows the spatial overlap of the predictive patterns relative to the different measures here employed. Results are superimposed on 3D T1 MRI template. FTD-*GRN*+, frontotemporal dementia carrying *Granulin* mutation; *aGRN*+, asymptomatic carriers of *Granulin* mutation.

should be used to achieve the best accuracy. In the present work, we took advantage of MVPA to concomitantly assess the utility of a series of MRI data in a cohort of *GRN* Thr272fs carriers, in their presymptomatic and symptomatic stages of the disease. The herein SVM approach was able to identify the optimal separation hyperplane (best accuracy) that maximized the separation between two given classes (i.e., FTD-*GRN*+ versus oHC or a*GRN*+ versus yHC), using either structural measures, such as grey and white matter density, and resting-state fMRI functional connectivity maps (such as functional networks or/and local connectivity maps). This allowed us to define which technique was the most useful in detecting significant

differences between groups and to identify the global pattern (rather than the significant clusters for the univariate approach) that best characterized and subsequently classified *GRN* carriers as compared to controls. In line with previous literature data, structural alterations were the most predictive measures when disease is overt, due to the neuronal loss and the disruption of white matter bundles [8, 17]. In this stage, we even found functional connectivity measure abnormalities, demonstrating both large-scale network disconnections and local within-network coherence hypoconnectivity [46, 47]. Overall, in symptomatic *GRN* mutation carriers, the brain damage was detected in the frontal, temporal and parietal regions, with a predominant involvement of left frontal and parietal areas. Furthermore, we were able to demonstrate that: 1) other functional networks beyond SN were involved in the clinical phase of FTD-*GRN*+ and 2) the best discriminative spatial pattern (for each of the studied measures) was characterized by areas of reduced connectivity as well as of increased connectivity, the latter with a potential compensatory role [20, 46]. Finally, local connectivity metrics supported the idea of a long-distance functional impairment coupled with grey matter atrophy in frontal, temporal and parietal regions.

Conversely, in the preclinical phase, structural changes were not able to identify *GRN* carriers accurately, while resting-state functional connectivity measures did. As compared to the results of the Genetic Fronto-temporal dementia Initiative (GENFI) study [17], we were not able to find any significant structural alteration in our sample of asymptomatic *GRN* carriers. This was probably due to the small sample size ($n = 17$) and to the mean age of our group, up to 10 years younger than that in GENFI study [17]. In our work, we found that local connectivity indexes, such as fALFF and DC, showed better classification performances than ICA networks measures. These local connectivity metrics captured the subtle perturbations of the local integration of the signal (namely focusing on the power of the signal as the sum of amplitudes in the low frequency oscillations, fALFF) [22], and the node characteristics that make a node "central" within a network, by counting the number of direct connections from each node to all others (DC) [23]. These abnormalities were indeed able not only to detect the alterations of a single network, but the impairment of the inter-correlation among the involved networks [48]. Interestingly, recent electrophysiological studies suggested that functional connectivity perturbation might be modulated, and might represent a target and a marker of disease-modifying therapies [49].

These data suggest that the early alterations in a*GRN*+ are represented by cumulative decreases in areas belonging to fronto-parietal regions with increased functional connectivity in prefrontal areas, measured by all local connectivity metrics and EN network. This was in line with our previous findings in *GRN*-related disease [9, 16, 20], demonstrating an impaired resting state functional connectivity in posterior regions as well as an increased (potentially compensatory) connectivity in prefrontal regions [50], in accordance with the concept of molecular nexopathies proposed by Warren et al. [51]. In this sense, in line with GENFI study [17], *GRN* disease is characterized by a progressive fronto-parietal impairment moving from preclinical to clinical stages, representing the pathological spreading of the disease following long-distance white matter bundles [51]. On the other hand, regions (i.e., prefrontal cortex) with a different profile of functional alteration during the *GRN* disease course, could reflect the complexity of brain dynamic interaction, with some regions with increased activity as compensatory effort towards damaged *at-distance* regions.

Our work argued for the usefulness of MVPA in identifying the most accurate neuroimaging marker for clinical trials in *GRN*-related disease, suggesting that functional connectivity metrics (i.e., local connectivity indexes) were the most accurate measures in preclinical phases, while structural (i.e., grey and white matter) alterations were the best tools when disease is overt. Furthermore, the best local connectivity measure (fALFF) in *aGRN*+ showed also high performances (total accuracy >80%) in discriminating FTD-*GRN*+ versus healthy controls. In this sense, throughout the application of MVPA, fALFF could be considered the best MRI marker in the *GRN* disease continuum. From this point of view, MVPA could be of help in describing the neuroimaging pattern of each stage of *GRN* disease: 1) an asymmetric pattern of frontal, temporal and parietal atrophy with a complex involvement of many functional brain networks in FTD-*GRN*+; and 2) a predominant involvement of functional brain networks, with a not well organized reduced connectivity in posterior regions associated with a high-structured increased activity in prefrontal regions in *aGRN*+.

However, our study presented several significant limitations. First of all, the cross-sectional evaluation of our samples (FTD-*GRN*+ and *aGRN*+) did not allow a complete understanding of the complex modulation of brain damage, especially for resting state

fMRI parameters. In this sense, multicenter longitudinal studies on genetically-defined populations are mandatory, in line with the aim of GENFI [17]. A further limitation, the sample size in the FTD-*GRN*+ group (16 patients, 8 bvFTD and 8 avPPA) did not allow a further evaluation of the functional and structural parameters of *GRN* mutation in the different clinical phenotypes; furthermore, as demonstrated by the analysis of the number of correct classifications for each subjects, in FTD-*GRN*+ the subject with the lowest number of correct classifications belonged to agrammatic variant of PPA, suggesting a partial inhomogeneity in FTD-*GRN*+ group. Moreover, nuisance variables inclusion in MVPA approach is not completely standardized, with multivariate analysis not controlled for age and education effects. Finally, despite high values of total accuracy, sensibility is approximately 70% and specificity 50%. In this regard, it is important to note that SVM was not originally defined to search for the best combination of sensitivity and specificity (like in receiver operating characteristic curve) but to define the best discrimination between two condition (or classes) [52]. Furthermore, in our work poor specificity could be primary due to a higher variability in yHC compared to *aGRN*+, considering the small sample size of the studied group. Considering SVM theoretical approach, this technique is optimized for groups with similar (or better identical) size, making the analysis of imbalanced groups problematic [52]. All these considerations partially weakening a direct clinical application of each single MRI index alone, supporting the idea of a global classifier to apply all the studied indexes at the same time.

Further studies are needed: 1) to simultaneously integrate all the aforementioned measures in a classifier able to trace the disease progression (increasing total accuracy, sensibility and specificity) moving from preclinical to clinical stage of the disease and 2) to integrate neuroimaging and biological markers in a multivariate statistical design ameliorating classification performances in *GRN*-related disease in monogenic and sporadic dementias. Furthermore, multivariate techniques like MVPA could be of interest in international multicenter study on *GRN* mutation as well as for other causative mutations for FTLD (*MAPT, C9orf72*).

ACKNOWLEDGMENTS

This project was funded by 26/RF-2010-2319722 grant (Italian NetALZ- DIAFN).

Authors' disclosures available online (http://j-alz.com/manuscript-disclosures/15-0340r2).

SUPPLEMENTARY MATERIAL

The supplementary material is available in the electronic version of this article: http://dx.doi.org/10.3233/JAD-150340.

REFERENCES

[1] Gorno-Tempini ML, Hillis AE, Weintraub S, Kertesz A, Mendez M, Cappa SF, Ogar JM, Rohrer JD, Black S, Boeve BF, Manes F, Dronkers NF, Vandenberghe R, Rascovsky K, Patterson K, Miller BL, Knopman DS, Hodges JR, Mesulam MM, Grossman M (2011) Classification of primary progressive aphasia and its variants. *Neurology* **76**, 1006-1014.

[2] Rascovsky K, Hodges JR, Knopman D, Mendez MF, Kramer JH, Neuhaus J, van Swieten JC, Seelaar H, Dopper EG, Onyike CU, Hillis AE, Josephs KA, Boeve BF, Kertesz A, Seeley WW, Rankin KP, Johnson JK, Gorno-Tempini ML, Rosen H, Prioleau-Latham CE, Lee A, Kipps CM, Lillo P, Piguet O, Rohrer JD, Rossor MN, Warren JD, Fox NC, Galasko D, Salmon DP, Black SE, Mesulam M, Weintraub S, Dickerson BC, Diehl-Schmid J, Pasquier F, Deramecourt V, Lebert F, Pijnenburg Y, Chow TW, Manes F, Grafman J, Cappa SF, Freedman M, Grossman M, Miller BL (2011) Sensitivity of revised diagnostic criteria for the behavioural variant of frontotemporal dementia. *Brain* **134**, 2456-2477.

[3] Rohrer JD, Warren JD, Modat M, Ridgway GR, Douiri A, Rossor MN, Ourselin S, Fox NC (2009) Patterns of cortical thinning in the language variants of frontotemporal lobar degeneration. *Neurology* **72**, 1562-1569.

[4] Whitwell JL, Josephs KA, Rossor MN, Stevens JM, Revesz T, Holton JL, Al-Sarraj S, Godbolt AK, Fox NC, Warren JD (2005) Magnetic resonance imaging signatures of tissue pathology in frontotemporal dementia. *Arch Neurol* **62**, 1402-1408.

[5] Mackenzie IR, Neumann M, Bigio EH, Cairns NJ, Alafuzoff I, Kril J, Kovacs GG, Ghetti B, Halliday G, Holm IE, Ince PG, Kamphorst W, Revesz T, Rozemuller AJ, Kumar-Singh S, Akiyama H, Baborie A, Spina S, Dickson DW, Trojanowski JQ, Mann DM (2010) Nomenclature and nosology for neuropathologic subtypes of frontotemporal lobar degeneration: An update. *Acta Neuropathol* **119**, 1-4.

[6] Rohrer JD, Lashley T, Schott JM, Warren JE, Mead S, Isaacs AM, Beck J, Hardy J, de Silva R, Warrington E, Troakes C, Al-Sarraj S, King A, Borroni B, Clarkson MJ, Ourselin S, Holton JL, Fox NC, Revesz T, Rossor MN, Warren JD (2011) Clinical and neuroanatomical signatures of tissue pathology in frontotemporal lobar degeneration. *Brain* **134**, 2565-2581.

[7] Rademakers R, Neumann M, Mackenzie IR (2012) Advances in understanding the molecular basis of frontotemporal dementia. *Nat Rev Neurol* **8**, 423-434.

[8] Whitwell JL, Jack CR Jr, Baker M, Rademakers R, Adamson J, Boeve BF, Knopman DS, Parisi JF, Petersen RC, Dickson DW, Hutton ML, Josephs KA (2007) Voxel-based morphometry in frontotemporal lobar degeneration with ubiquitin-positive inclusions with and without progranulin mutations. *Arch Neurol* **64**, 371-376.

[9] Borroni B, Alberici A, Cercignani M, Premi E, Serra L, Cerini C, Cosseddu M, Pettenati C, Turla M, Archetti S, Gasparotti R,

Caltagirone C, Padovani A, Bozzali M (2012) Granulin mutation drives brain damage and reorganization from preclinical to symptomatic FTLD. *Neurobiol Aging* **33**, 2506-2520.

[10] Whitwell JL, Jack CR Jr, Boeve BF, Senjem ML, Baker M, Rademakers R, Ivnik RJ, Knopman DS, Wszolek ZK, Petersen RC, Josephs KA (2009) Voxel-based morphometry patterns of atrophy in FTLD with mutations in MAPT or PGRN. *Neurology* **72**, 813-820.

[11] Habeck CG (2010) Basics of multivariate analysis in neuroimaging data. *J Vis Exp*, pii: 1988. doi: 10.3791-1988

[12] Davis T, LaRocque KF, Mumford JA, Norman KA, Wagner AD, Poldrack RA (2014) What do differences between multi-voxel and univariate analysis mean? How subject-, voxel-, and trial-level variance impact fMRI analysis. *Neuroimage* **97**, 271-283.

[13] Coutanche MN, Thompson-Schill SL, Schultz RT (2011) Multi-voxel pattern analysis of fMRI data predicts clinical symptom severity. *Neuroimage* **57**, 113-123.

[14] Moradi E, Pepe A, Gaser C, Huttunen H, Tohka J, Alzheimer's Disease Neuroimaging Initiative (2015) Machine learning framework for early MRI-based Alzheimer's conversion prediction in MCI subjects. *Neuroimage* **104**, 398-412.

[15] Bron EE, Steketee RM, Houston GC, Oliver RA, Achterberg HC, Loog M, van Swieten JC, Hammers A, Niessen WJ, Smits M, Klein S (2014) Diagnostic classification of arterial spin labeling and structural MRI in presenile early stage dementia. *Hum Brain Mapp* **35**, 4916-4931.

[16] Premi E, Cauda F, Gasparotti R, Diano M, Archetti S, Padovani A, Borroni B (2014) Multimodal FMRI resting-state functional connectivity in granulin mutations: The case of fronto-parietal dementia. *PLoS One* **9**, e106500.

[17] Rohrer JD, Nicholas JM, Cash DM, van Swieten J, Dopper E, Jiskoot L, van Minkelen R, Rombouts SA, Cardoso MJ, Clegg S, Espak M, Mead S, Thomas DL, De Vita E, Masellis M, Black SE, Freedman M, Keren R, MacIntosh BJ, Rogaeva E, Tang-Wai D, Tartaglia MC, Laforce R Jr, Tagliavini F, Tiraboschi P, Redaelli V, Prioni S, Grisoli M, Borroni B, Padovani A, Galimberti D, Scarpini E, Arighi A, Fumagalli G, Rowe JB, Coyle-Gilchrist I, Graff C, Fallstrom M, Jelic V, Stahlbom AK, Andersson C, Thonberg H, Lilius L, Frisoni GB, Pievani M, Bocchetta M, Benussi L, Ghidoni R, Finger E, Sorbi S, Nacmias B, Lombardi G, Polito C, Warren JD, Ourselin S, Fox NC, Rossor MN (2015) Presymptomatic cognitive and neuroanatomical changes in genetic frontotemporal dementia in the Genetic Frontotemporal dementia Initiative (GENFI) study: A cross-sectional analysis. *Lancet Neurol* **14**, 253-262.

[18] Jack CR Jr, Knopman DS, Jagust WJ, Petersen RC, Weiner MW, Aisen PS, Shaw LM, Vemuri P, Wiste HJ, Weigand SD, Lesnick TG, Pankratz VS, Donohue MC, Trojanowski JQ (2013) Tracking pathophysiological processes in Alzheimer's disease: An updated hypothetical model of dynamic biomarkers. *Lancet Neurol* **12**, 207-216.

[19] Ashburner J, Friston KJ (2000) Voxel-based morphometry–the methods. *Neuroimage* **11**, 805-821.

[20] Premi E, Formenti A, Gazzina S, Archetti S, Gasparotti R, Padovani A, Borroni B (2013) Effect of TMEM106B polymorphism on functional network connectivity in asymptomatic GRN mutation carriers. *JAMA Neurol* **71**, 216-221.

[21] Zhang Z, Liu Y, Jiang T, Zhou B, An N, Dai H, Wang P, Niu Y, Wang L, Zhang X (2012) Altered spontaneous activity in Alzheimer's disease and mild cognitive impairment revealed by Regional Homogeneity. *Neuroimage* **59**, 1429-1440.

[22] Zou QH, Zhu CZ, Yang Y, Zuo XN, Long XY, Cao QJ, Wang YF, Zang YF (2008) An improved approach to detection of amplitude of low-frequency fluctuation (ALFF) for resting-state fMRI: Fractional ALFF. *J Neurosci Methods* **172**, 137-141.

[23] Buckner RL, Sepulcre J, Talukdar T, Krienen FM, Liu H, Hedden T, Andrews-Hanna JR, Sperling RA, Johnson KA (2009) Cortical hubs revealed by intrinsic functional connectivity: Mapping, assessment of stability, and relation to Alzheimer's disease. *J Neurosci* **29**, 1860-1873.

[24] Zuo XN, Kelly C, Di Martino A, Mennes M, Margulies DS, Bangaru S, Grzadzinski R, Evans AC, Zang YF, Castellanos FX, Milham MP (2010) Growing together and growing apart: Regional and sex differences in the lifespan developmental trajectories of functional homotopy. *J Neurosci* **30**, 15034-15043.

[25] Borroni B, Agosti C, Premi E, Cerini C, Cosseddu M, Paghera B, Bellelli G, Padovani A (2010) The FTLD-modified Clinical Dementia Rating scale is a reliable tool for defining disease severity in frontotemporal lobar degeneration: Evidence from a brain SPECT study. *Eur J Neurol* **17**, 703-707.

[26] Borroni B, Alberici A, Premi E, Archetti S, Garibotto V, Agosti C, Gasparotti R, Di Luca M, Perani D, Padovani A (2008) Brain magnetic resonance imaging structural changes in a pedigree of asymptomatic progranulin mutation carriers. *Rejuvenation Res* **11**, 585-595.

[27] Chao-Gan Y, Yu-Feng Z (2010) DPARSF: A MATLAB toolbox for "Pipeline" Data analysis of resting-state fMRI. *Front Syst Neurosci* **4**, 13.

[28] Song XW, Dong ZY, Long XY, Li SF, Zuo XN, Zhu CZ, He Y, Yan CG, Zang YF (2011) REST: A toolkit for resting-state functional magnetic resonance imaging data processing. *PLoS One* **6**, e25031.

[29] Mourao-Miranda J, Bokde AL, Born C, Hampel H, Stetter M (2005) Classifying brain states and determining the discriminating activation patterns: Support vector machine on functional MRI data. *Neuroimage* **28**, 980-995.

[30] Peelen MV, Downing PE (2007) Using multi-voxel pattern analysis of fMRI data to interpret overlapping functional activations. *Trends Cogn Sci* **11**, 4-5.

[31] Boser BE, Guyon IM, Vapnik VN (1992) A training algorithm for optimal margin classifiers. *In Proceedings of the 5th Annual Workshop on Computational Learning Theory ACM*, Pittsburgh, Pennsylvania, USA, pp. 144-152.

[32] De Martino F, Valente G, Staeren N, Ashburner J, Goebel R, Formisano E (2008) Combining multivariate voxel selection and support vector machines for mapping and classification of fMRI spatial patterns. *Neuroimage* **43**, 44-58.

[33] Esterman M, Tamber-Rosenau BJ, Chiu YC, Yantis S (2010) Avoiding non-independence in fMRI data analysis: Leave one subject out. *Neuroimage* **50**, 572-576.

[34] Bishop C (2006) *Pattern Recognition and Machine Learning*, Springer-Verlag New York, New York.

[35] Chih-Chung Chang C-JL (2001) LIBSVM: A library for support vector machines. *ACM Transactions on Intelligent Systems and Technology* **27**.

[36] Filippini N, MacIntosh BJ, Hough MG, Goodwin GM, Frisoni GB, Smith SM, Matthews PM, Beckmann CF, Mackay CE (2009) Distinct patterns of brain activity in young carriers of the APOE-epsilon4 allele. *Proc Natl Acad Sci U S A* **106**, 7209-7214.

[37] Karageorgiou E, Miller BL (2014) Frontotemporal lobar degeneration: A clinical approach. *Semin Neurol* **34**, 189-201.

[38] Boxer AL, Gold M, Huey E, Gao FB, Burton EA, Chow T, Kao A, Leavitt BR, Lamb B, Grether M, Knopman D, Cairns NJ, Mackenzie IR, Mitic L, Roberson ED, Van Kammen D, Cantillon M, Zahs K, Salloway S, Morris J, Tong G, Feldman H, Fillit H, Dickinson S, Khachaturian Z, Sutherland M, Farese

R, Miller BL, Cummings J (2013) Frontotemporal degeneration, the next therapeutic frontier: Molecules and animal models for frontotemporal degeneration drug development. *Alzheimers Dement* **9**, 176-188.

[39] Josephs KA, Hodges JR, Snowden JS, Mackenzie IR, Neumann M, Mann DM, Dickson DW (2011) Neuropathological background of phenotypical variability in frontotemporal dementia. *Acta Neuropathol* **122**, 137-153.

[40] D'Alton S, Lewis J (2014) Therapeutic and diagnostic challenges for frontotemporal dementia. *Front Aging Neurosci* **6**, 204.

[41] Alberici A, Archetti S, Pilotto A, Premi E, Cosseddu M, Bianchetti A, Semeraro F, Salvetti M, Muiesan ML, Padovani A, Borroni B (2014) Results from a pilot study on amiodarone administration in monogenic frontotemporal dementia with granulin mutation. *Neurol Sci* **35**, 1215-1219.

[42] Kumar-Singh S (2011) Progranulin and TDP-43: Mechanistic links and future directions. *J Mol Neurosci* **45**, 561-573.

[43] Kleinberger G, Capell A, Haass C, Van Broeckhoven C (2013) Mechanisms of granulin deficiency: Lessons from cellular and animal models. *Mol Neurobiol* **47**, 337-360.

[44] Dopper EG, Rombouts SA, Jiskoot LC, Heijer T, de Graaf JR, Koning I, Hammerschlag AR, Seelaar H, Seeley WW, Veer IM, van Buchem MA, Rizzu P, van Swieten JC (2013) Structural and functional brain connectivity in presymptomatic familial frontotemporal dementia. *Neurology* **80**, 814-823.

[45] Pievani M, Filippini N, van den Heuvel MP, Cappa SF, Frisoni GB (2014) Brain connectivity in neurodegenerative diseases-from phenotype to proteinopathy. *Nat Rev Neurol* **10**, 620-633.

[46] Zhou J, Greicius MD, Gennatas ED, Growdon ME, Jang JY, Rabinovici GD, Kramer JH, Weiner M, Miller BL, Seeley WW (2010) Divergent network connectivity changes in behavioural variant frontotemporal dementia and Alzheimer's disease. *Brain* **133**, 1352-1367.

[47] Filippi M, Agosta F, Scola E, Canu E, Magnani G, Marcone A, Valsasina P, Caso F, Copetti M, Comi G, Cappa SF, Falini A (2013) Functional network connectivity in the behavioral variant of frontotemporal dementia. *Cortex* **49**, 2389-2401.

[48] Cabral J, Hugues E, Sporns O, Deco G (2011) Role of local network oscillations in resting-state functional connectivity. *Neuroimage* **57**, 130-139.

[49] Fox MD, Halko MA, Eldaief MC, Pascual-Leone A (2012) Measuring and manipulating brain connectivity with resting state functional connectivity magnetic resonance imaging (fcMRI) and transcranial magnetic stimulation (TMS). *Neuroimage* **62**, 2232-2243.

[50] Farb NA, Grady CL, Strother S, Tang-Wai DF, Masellis M, Black S, Freedman M, Pollock BG, Campbell KL, Hasher L, Chow TW (2013) Abnormal network connectivity in frontotemporal dementia: Evidence for prefrontal isolation. *Cortex* **49**, 1856-1873.

[51] Warren JD, Rohrer JD, Schott JM, Fox NC, Hardy J, Rossor MN (2013) Molecular nexopathies: A new paradigm of neurodegenerative disease. *Trends Neurosci* **36**, 561-569.

[52] Veropoulos K, Campbell C, Cristianini N (1999) Controlling the sensitivity of support vector machines. *In Proceedings of the International Joint Conference on AI*, pp. 55-60.